



SERENDIPITOUS DISCOVERY OF A PROJECTED PAIR OF QSOs SEPARATED BY 4.5 arcsec ON THE SKY*

K. E. HEINTZ^{1,10}, J. P. U. FYNBO¹, J.-K. KROGAGER^{1,6}, M. VESTERGAARD^{1,2}, P. MØLLER³, M. ARABSALMANI³, S. GEIER^{4,5},
P. NOTERDAEME⁶, C. LEDOUX⁷, F. G. SATURNI⁸, AND B. VENEMANS⁹

¹ Dark Cosmology Centre, Niels Bohr Institute, University of Copenhagen, Juliane Maries Vej 30, DK-2100 Copenhagen O, Denmark; heintz@dark-cosmology.dk

² Steward Observatory, University of Arizona, 933 N. Cherry Avenue, Tucson AZ 85721, USA

³ European Southern Observatory, Karl-Schwarzschildstrasse 2, D-85748 Garching, Germany

⁴ Gran Telescopio Canarias (GRANTECAN), Cuesta de San José s/n, E-38712, Breña Baja, La Palma, Spain

⁵ Instituto de Astrofísica de Canarias, Vía Láctea s/n, E-38200, La Laguna, Tenerife, Spain

⁶ Institut d’Astrophysique de Paris, CNRS-UPMC, UMR7095, 98bis bd Arago, F-75014 Paris, France

⁷ European Southern Observatory, Alonso de Crdova 3107, Vitacura, Casilla 19001, Santiago 19, Chile

⁸ University of Rome “La Sapienza”, p.le A. Moro 5, I-00185 Rome, Italy

⁹ Max-Planck Institute for Astronomy, Königstuhl 17, D-69117 Heidelberg, Germany

Received 2016 February 16; accepted 2016 April 15; published 2016 June 21

ABSTRACT

We present the serendipitous discovery of a projected pair of quasi-stellar objects (QSOs) with an angular separation of $\Delta\theta = 4.50$ arcsec. The redshifts of the two QSOs are widely different: one, our program target, is a QSO with a spectrum consistent with being a narrow line Seyfert 1 active galactic nucleus at $z = 2.05$. For this target we detect Ly α , C IV, and C III]. The other QSO, which by chance was included on the spectroscopic slit, is a Type 1 QSO at a redshift of $z = 1.68$, for which we detect C IV, C III], and Mg II. We compare this system to previously detected projected QSO pairs and find that only about a dozen previously known pairs have smaller angular separation.

Key words: quasars: general

1. INTRODUCTION

We report the discovery of a closely projected pair of quasi-stellar objects (QSOs) with an angular separation of only $\Delta\theta = 4.50$ arcsec. The observing run from which the spectra of these two objects were obtained was unrelated to the search for close projected QSO pairs. Originally, the run was designed to spectroscopically verify candidate dust-reddened QSOs, as part of the High A_V Quasar (HAQ) survey (Fynbo et al. 2013; Krogager et al. 2015). The dust-reddened candidate QSO originally intended to be verified spectroscopically, HAQ2358+1030A, J2000 coordinates $\alpha_A = 23^{\text{h}} 58^{\text{m}} 40^{\text{s}}.47$, $\delta_A = +10^{\circ} 30^{\text{m}} 40^{\text{s}}.07$, will henceforth just be denoted as object A. The companion “HAQ”2358+1030B with J2000 coordinates ($\alpha_B = 23^{\text{h}} 58^{\text{m}} 40^{\text{s}}.53$, $\delta_B = +10^{\circ} 30^{\text{m}} 35^{\text{s}}.53$, will be denoted as object B. The companion QSO was discovered serendipitously, coincidentally placed on the slit during the target acquisition of object A. The slit was aligned at the parallactic angle.

The small angular separation of this projected pair of QSOs is quite unusual and will be discussed briefly in Section 4. Previously, Hennawi et al. (2006b) carried out an extensive search for binary QSO systems, using the Sloan Digital Sky Survey (SDSS; York et al. 2000) and the 2dF QSO Redshift Survey (2QZ; Croom et al. 2004) QSO catalogs. They primarily focused on selecting binary QSO pairs, the controversial population discovered in the search for small-scale $2 \leq \Delta\theta \leq 10$ arcsec gravitationally lensed QSOs (e.g., Mortlock et al. 1999), to study the small-scale QSO clustering

and correlation function. However, the majority of the detected QSO pair systems were projected systems, having relative radial separations of $\Delta z \approx 0.3\text{--}1.0$. The discovery of these close angularly separated projected QSO pairs initiated the search and study of “quasars probing quasars” (see e.g., Hennawi et al. 2006a, and later papers). Close binary QSOs and projected QSO pairs are important for studies of small-scale QSO clustering, the tomography of the inter-galactic medium along close lines of sight, the effects of QSO transverse ionization (Møller & Kjaergaard 1992), and gravitationally lensed QSOs.

Throughout this paper we assume the standard Λ CDM cosmology with $H_0 = 70 \text{ km s}^{-1} \text{ Mpc}^{-1}$, $\Omega_M = 0.28$, and $\Omega_\Lambda = 0.72$ (Komatsu et al. 2011).

2. OBSERVATIONS

In Figure 1 we present a 1×1 arcmin² field around the two sources (marked A and B) as imaged in the *i*-band by SDSS in Data Release 12 (DR12) (Alam 2015).

The observation was carried out during an observing run with the Nordic Optical Telescope (NOT) on La Palma in 2015 September. The spectra were obtained using the Andalucia Faint Object Spectrograph and Camera (ALFOSC), grism #4 covering the wavelengths 3200–9100 Å (with a spectral resolution of 21 Å) and a slit width of 1.3 arcsec. Blocking filter #94 was used in order to prevent second-order contamination from wavelengths shorter than 3560 Å. Two exposures of 1200 s were taken. The object south of our program target is the one captured serendipitously.

One additional spectrum was taken on 2016 January 9 in a redder grism (grism #20). This spectrum was taken again with a position angle covering both QSOs. A total exposure time of 3200 s was secured. The purpose of this spectrum was to confirm that an unidentified emission line in the spectrum of object A was due to second-order contamination (see below).

* Based on observations made with the Nordic Optical Telescope, on the island of La Palma jointly operated by Denmark, Finland, Iceland, Norway, and Sweden, in the Spanish Observatorio del Roque de los Muchachos of the Instituto de Astrofísica de Canarias.

¹⁰ Author to whom correspondence should be addressed.

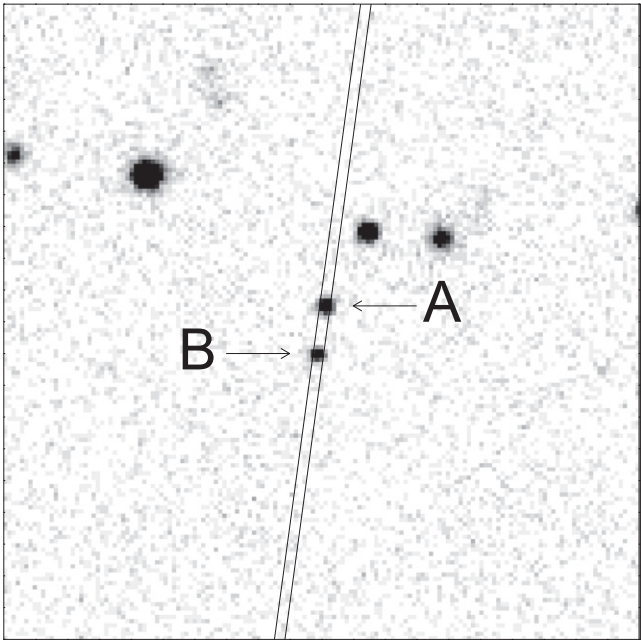


Figure 1. A 1×1 arcmin² field around the two sources (marked A and B) as imaged in the *i*-band by SDSS DR12. North is up and east is to the left. A schematic view of the actual slit, used during the observation, which was centered on source A and aligned with the parallactic angle ($-7^{\circ}7'$ east of north (EoN) at the time) is shown. The position angle between the two objects is $-10^{\circ}1'$ EoN.

The spectra were processed using a combination of IRAF¹¹ and MIDAS¹² tasks for low resolution spectroscopy. To reject cosmic rays we used `La_cosmic` (van Dokkum 2001). We corrected the spectra for Galactic extinction using the extinction maps of Schlegel et al. (1998). To improve the absolute flux calibration we scaled the spectra to be consistent with the *r*-band photometry from SDSS.

3. THE PROJECTED QSO PAIR HAQ2358+1030A AND B

The projected angular separation between the two objects is ~ 4.6 arcsec as measured on the SDSS images.¹³ Based on the acquisition picture obtained we find a projected angular separation of only 23.5 pixels = 4.50 arcsec (0.19 arcsec/pixel for ALFOSC). This corresponds to a physical angular separation of 39.2 kpc at $z = 1.5$. Since our measurement is taken directly from the acquisition picture, we consider this a more precise estimate of the angular separation of the two objects due to the better spatial resolution in these data.

Figure 2 shows the two one-dimensional spectra after flat-field correction, bias and sky subtraction, and flux calibration along with the photometry from SDSS and the UKIRT Infrared Deep Sky Survey (UKIDSS; Lawrence et al. 2007) which are all on the AB magnitude system. We determine the redshift by visual inspection of the emission lines visible in the spectra.

¹¹ IRAF is the Image Reduction and Analysis Facility, a general purpose software system for the reduction and analysis of astronomical data. IRAF is written and supported by the National Optical Astronomy Observatories (NOAO) in Tucson, Arizona. NOAO is operated by the Association of Universities for Research in Astronomy (AURA), Inc. under cooperative agreement with the National Science Foundation

¹² ESO-MIDAS is a copyright protected software product of the European Southern Observatory. The software is available under the GNU General Public License.

¹³ <http://skyserver.sdss.org/dr12/en/tools/explore/Summary.aspx?>

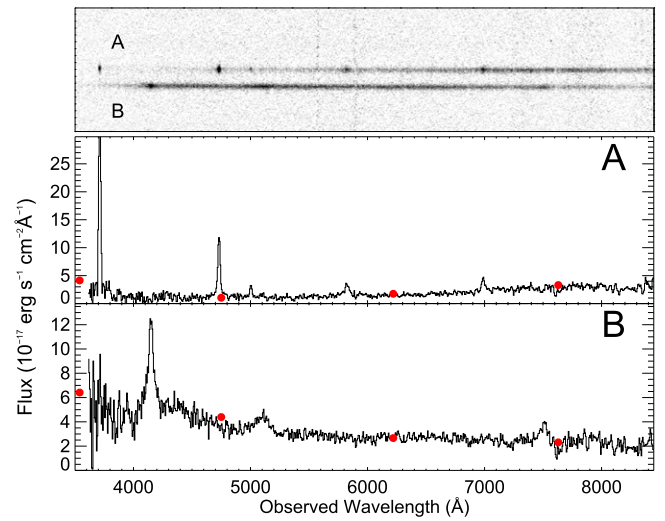


Figure 2. Top panel: the 2D spectrum showing the traces of the two sources marked with A and B. Middle and bottom panels: the 1D spectra of the two sources. The observed spectra are plotted as the solid black lines and the photometric data points from SDSS are shown as the red dots (left to right: *u*, *g*, *r*, *i*). The spectra have been scaled to match the *r*-band photometric data point from SDSS. Object A is a QSO equivalent of a narrow line Seyfert 1 galaxy at $z = 2.05$ whereas B is a Type 1 QSO at $z = 1.68$.

Table 1 lists the optical and near-infrared AB magnitudes for each of the two objects from the SDSS DR12 and the UKIDSS DR10plus catalogs.

In Table 2 we list the wavelengths, line widths (full width at half maximum, FWHM), and derived redshifts for the detected emission lines for the two objects. Object A is identified as a dust-reddened QSO equivalent of a narrow line Seyfert 1 galaxy classified by its narrow C IV $\lambda 1549$ emission line with a FWHM of 920 km s^{-1} . The redshift is determined to be $z = 2.053$ based on the visible Ly α and the C IV, C III] $\lambda 1909$ emission lines. There is an additional emission line in this spectrum at rest wavelength 2289 Å. This line is not prominent in the the empirical ultraviolet template for iron emission in active galactic nucleus derived from I Zwicky 1 (Vestergaard & Wilkes 2001) and we have not been able to find it in other spectra for QSOs in the literature. The new spectrum obtained in 2016 January at the NOT with grism #20 confirms that this line is due to second-order contamination (Stanishev 2007) and is hence not real.

The reddening of this object was determined to be $A_V = 1.1$ from the photometric data points and the shape of the continuum following the procedure of Fynbo et al. (2013) and Krogager et al. (2015). Object B is identified to be a regular, unreddened Type 1 QSO with a FWHM of 4200 km s^{-1} of the C IV emission line. The redshift was determined to be $z = 1.68$ based on the broad C IV and C III] emission lines. The unobscured nature of this object was again determined from the photometric data points and the shape of the continuum.

The redshift measurements suggest a relative radial distance of $\Delta z = 0.38$ between the two QSOs. Only about a dozen other systems of projected QSO pairs with $\Delta\theta < 4.50$ arcsec have been reported in the systematic search by Hennawi et al. (2006a, see Tables 8 and 9), Inada et al. (2012), and More et al. (2016), all with relative radial distances $\Delta z \sim 0.3-1.1$. It is also worth noting that neither of these two QSOs are included in the DR12 QSO survey. We selected object A as a candidate dust-

Table 1
The Optical and Near-infrared Magnitudes of Objects A and B all on the AB Magnitude System from the SDSS and UKIDSS Catalogs

Object	u (mag)	g (mag)	r (mag)	i (mag)	z (mag)	Y (mag)	J (mag)	H (mag)	K_s (mag)
A	21.37	22.10	20.82	19.62	18.92	18.62	18.21	17.71	17.24
B	20.90	20.54	20.37	20.01	20.01	20.06	20.07	19.74	19.71

Table 2
Wavelength, Line Widths (Measured and Corrected for the Spectral Resolution), and Derived Redshifts for all Detected Emission Lines

Line	λ_{obs} (Å)	FWHM (Å)	FWHM _{corr} (Å)	z
Object A				
Ly α λ 1216	3711.8 ± 0.5	20.0 ± 1.2	12.3 ± 1.2	2.0533 ± 0.0004
C IV λ 1549	4731.0 ± 0.4	24.8 ± 0.9	14.5 ± 0.9	2.0533 ± 0.0004
He II λ 1640	5003.7 ± 1.3	20.0 ± 0.9	...	2.0503 ± 0.0008
C III] λ 1909	5825.1 ± 1.8	43.1 ± 4.5	35.3 ± 4.5	2.0530 ± 0.0008
Ly α 2nd order λ 2289	6989.7 ± 1.4	36.2 ± 3.4	20.7 ± 3.4	2.053
Object B				
C IV λ 1549	4149.7 ± 1.7	61.0 ± 4.1	58.4 ± 4.1	1.6781 ± 0.0011
C III] λ 1909	5100.8 ± 5.8	124.4 ± 14.4	122.5 ± 14.4	1.673 ± 0.003
Mg II λ 2800	7506.4 ± 3.8	63.1 ± 10.1	54.5 ± 10.1	1.6817 ± 0.0014

reddened QSO in the HAQ survey (see e.g., Fynbo et al. 2013; Krogager et al. 2015). Object B evaded selection due to its specific photometry falling outside the selection criteria of BOSS, which is optimized for $z > 2$.

We looked for associated absorption in the two spectra, more specifically absorption in the spectrum of object A due to, e.g., Mg II λ 2800 or C IV due to gas associated with the foreground QSO object B. The continuum level in the spectrum of A is too weak at the position of C IV at the redshift of object B to allow detection of absorption. For Mg II we show the relevant spectral regions in Figure 3. There is a hint of Mg II absorption at 7490.2 Å with an observed equivalent width of 8 ± 3 Å found by integrating the error spectrum across the absorption line extent. This wavelength corresponds to $z_{\text{abs}} = 1.676$, roughly consistent, but slightly blueshifted, relative to the expected position at the redshift of object B.

4. THE SIGNIFICANCE OF CLOSELY SEPARATED QSO PAIRS

The projected pair of close angularly separated QSOs is a rare finding. Richards et al. (2005) find an integrated space density of QSOs brighter than $g = 20.5$ (brightness of object B) of $\sim 31 \text{ deg}^{-2}$ based on the 2dF-SDSS LRG and QSO (2SLAQ) survey. This intrinsic number density is based on robust optical five-band (u, g, r, i, z) color-color cuts similar to those utilized in the first SDSS QSO selection algorithm (Richards et al. 2002) although with slight modifications for the faintest objects. Based on the integrated space density, we estimated the likelihood of observing one additional QSO in the slit placed on object A. Considering only QSO pairs where (as in our case) the redshift difference corresponds to a distance much larger than the two-point correlation length, then the likelihood can be calculated as

$$\sim (31/3600/3600) \times 1.3 \times 10 \approx 3.1 \times 10^{-5}, \quad (1)$$

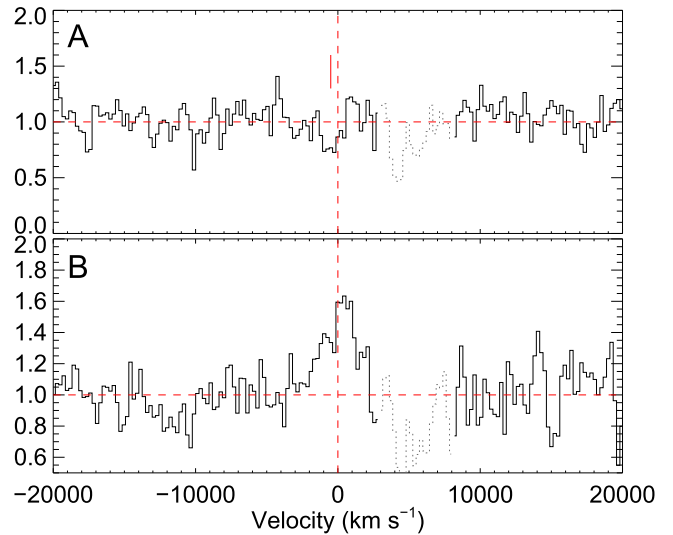


Figure 3. This figure shows the normalized spectra of object A and B in the regions around Mg II at the redshift of object B. In the top panel there is a hint of Mg II absorption with a formal significance of about 3σ . The part of the spectra shown in dotted gray represents telluric absorption.

where the last two numbers are the width of the slit and the length within which object B was detected ($\sim 2 \times 5$ arcsec) from object A, respectively. Had the observation been carried out just an hour later, the parallactic angle of the slit would not have captured this nearby companion, and we would not have discovered this system. When extrapolating the conservative total number of QSOs in the sky of $\sim 31 \times 41.253 \text{ deg}^2 \approx 1.3 \times 10^6$ and using the estimate of the likelihood per square degree we compute how many such cases on the entire sky is expected. We found a total of only ~ 140 cases of such closely separated QSO systems within the magnitude limit of object B. This detection was indeed serendipitous.

We wish to thank the anonymous referee for the helpful comments that improved the quality of this work. The research leading to these results has received funding from the European Research Council under the European Union's Seventh Framework Program (FP7/2007-2013)/ERC Grant agreement No. EGGS-278202. The data presented here were obtained with ALFOSC, which is provided by the Instituto de Astrofísica de Andalucía (IAA) under a joint agreement with the University of Copenhagen and NOTSA. B.V. acknowledges funding through the ERC grant Cosmic Dawn. M.V. gratefully acknowledges support from the Danish Council for Independent Research via grant No. DFF 4002-00275. Funding for the Sloan Digital Sky Survey III has been provided by the Alfred P. Sloan Foundation, the U.S. Department of Energy Office of Science, and the Participating Institutions. SDSS-IV acknowledges support and resources from the Center for High-Performance Computing at the University of Utah. The SDSS website is www.sdss.org.

REFERENCES

- Alam, S., Albareti, F. D., Allende Prieto, C., et al. 2015, *ApJS*, 219, 12
Croom, S. M., Smith, R. J., Boyle, B. J., et al. 2004, *MNRAS*, 349, 1397
Fynbo, J. P. U., Krogager, J.-K., Venemans, B., et al. 2013, *ApJS*, 204, 6
Hennawi, J. F., Prochaska, J. X., Burles, S., et al. 2006a, *ApJ*, 651, 61
Hennawi, J. F., Strauss, M. A., Oguri, M., et al. 2006b, *AJ*, 131, 1
Inada, N., Oguri, M., Shin, M.-S., et al. 2012, *AJ*, 143, 119
Komatsu, E., Smith, K. M., Dunkley, J., et al. 2011, *ApJS*, 192, 18
Krogager, J.-K., Geier, S., Fynbo, J. P. U., et al. 2015, *ApJS*, 217, 5
Lawrence, A., Warren, S. J., Almaini, O., et al. 2007, *MNRAS*, 379, 1599
Møller, P., & Kjaergaard, P. 1992, *A&A*, 258, 234
More, A., Oguri, M., Kayo, I., et al. 2016, *MNRAS*, 456, 1595
Mortlock, D. J., Webster, R. L., & Francis, P. J. 1999, *MNRAS*, 309, 836
Richards, G. T., Croom, S. M., Anderson, S. F., et al. 2005, *MNRAS*, 360, 839
Richards, G. T., Fan, X., Newberg, H. J., et al. 2002, *AJ*, 123, 2945
Schlegel, D. J., Finkbeiner, D. P., & Davis, M. 1998, *ApJ*, 500, 525
Stanishev, V. 2007, *AN*, 328, 948
van Dokkum, P. G. 2001, *PASP*, 113, 1420
Vestergaard, M., & Wilkes, B. J. 2001, *ApJS*, 134, 1
York, D. G., Adelman, J., Anderson, J. E., Jr., et al. 2000, *AJ*, 120, 1579